AIMS Energy, 11(3): 555–575.
DOI: 10.3934/energy.2023029
Received: 15 February 2023
Revised: 21 May 2023
Accepted: 23 May 2023
Published: 15 June 2023

http://www.aimspress.com/journal/energy

Research article

Analytical assessment of the filed results on the PV system connectors performance under operating temperature

Mebarek LAHBIB[1], Mohammed BOUSSAID[1], Houcine MOUNGAR[2] and Ahmed TAHRI[2,*]

[1] Laboratory of energy, environment and information systems, Department of Material Sciences, University of Ahmed Draia, Adrar, Algeria
[2] Renewable Energy Research Unit in Saharan Area (URERMS), Renewable Energy Development Center (CDER), Adrar, Algeria

* **Correspondence:** Email: tahrimoulayahmed@gmail.com; Tel: +2130663878885; Fax: +21349632249.

Abstract: In this study, we will shed light on the aggressive effect of a blowing sandstorm in the presence of high temperatures on the photovoltaic inter-module connectors in a solar station located in the desert environment of southwestern Algeria. After a short period of operation, it is observed that the MC4 connectors, which tighten the interconnection between the photovoltaic modules, are completely faulty because of sand grains carried away by a wind blowing at an average annual speed, which exceeds 6 m/s. Then, we analyzed and evaluated the connector failure to propose an appropriate solution. We checked the variations of the intrinsic temperatures of each connector employing the thermocouple for the three cases of operating temperatures, as well as the current measurement flowing through each connector, to calculate the powers dissipated in each branch of the circuit. Finally, this experimental work shows that a loss of power reaches almost 10% from the nominal power of the typical case. The proposed solution for this problem is to cover the connectors with an impervious plastic cover.

Keywords: solar station; temperature; energy; connector of modules; sand wind

1. Introduction

Of all the renewable energies, solar photovoltaic is of particular interest for the countries of the greater Sahara Desert since it has a solar deposit that is conducive to the development of this form of energy. At the end of 2015, the installed cumulative global capacity was estimated at 228 GW according to the International Energy Agency [1,2]. The performance of the photovoltaic modules depends on the environmental conditions. The energy efficiency proportionally increases to the irradiation and inversely to the temperature of the photovoltaic module [3,4]. Several studies have been conducted on the performance evaluation and analysis of the degradation of various solar photovoltaic power plants installed in the world. Khanam et al. (2021) evaluated and compared the performance of monocrystalline, polycrystalline, and thin film modules in four climatic zones of India (New Delhi, Srinagar, Bangalore, and Jodhpur). The obtained results showed that the efficiency of photovoltaic modules does not mainly depend on the intensity of received solar radiation but is strongly influenced by the peak temperatures of photovoltaic modules [5–7]. Aboagye et al. (2021) quantified the degradation rates and predicted the lifetime of 16 photovoltaic systems of different technologies that were installed in different locations in Ghana. The results revealed that the crystalline silicon modules degraded less than the amorphous silicon ones. Overall, the median and average expected lifetime of PV systems (crystalline and amorphous silicon) were 14 years and 16 years, respectively [8,9]. For 12 months, Dahbi et al. (2021) analyzed and studied a six MW photovoltaic power plant that was connected to the network and installed on a terrestrial base in Zaouit-Konta (27°13 00" N, 0°12 00" W). They noticed that the performance ratio linearly decreases with either an increasing ambient temperature or solar irradiation. An increase in ambient temperature and irradiation of 1°C and 10 Wh/m^2 leads to a decrease in the performance ratio of up to 2.7% and 0.11%, respectively [10,11]. Boussaid et al. (2016) experimentally verified the degradation of modules that were exposed to sunlight in an open circuit in a desert environment of those connected to adequate loads. For this purpose, the lifespan could be reduced to 4 years [12]. Ali Sadat et al. (2021) studied the effect of dust on the energy efficiency of solar photovoltaic modules in a desert region of Iran. They observed that the conversion efficiency, the normalized maximum power, the open circuit current, and the short circuit current decreased by 98.2%, 98.13%, 20.63%, and 98.02%, respectively [13,14]. Using a new model, Jing et al. (2016) estimated the frequency of cleaning photovoltaic modules in desert areas when the energy reduction and the concentration of particles are 5% and 100 μg/m^3, respectively, where it ultimately took about 20 days [15].

Benabdelkrim et al. [16] conducted an experimental study to analyze the PV station performance of a field-exposed polycrystalline silicon photovoltaic system using monitored data and the installed PV plant capacity of 20 MW that operates in the arid climate of southern Algeria in Adrar city. They concluded that the expected energy outputs decrease in a few months (generally from May to September) due to the influence of meteorological parameters, in particular the temperatures of the modules and other components. This corresponds to efficiencies of the PV system between 8.92% (in June) and 11.93% (in January) due to the temperature. Abdulrahman et al. [17] investigated a numerical analysis with an experimental demonstration to analyze the temperature's effect on the performance of the PV module. They simulated that the module temperature (25 to 65 ℃) influences the current-voltage I-V and power-voltage P-V under the Iraq weather conditions. Muzaffar Ali et al. [18] conducted an experimental prosses to investigate the performance of two panels according to the real climatic conditions at Taxila city in Pakistan. Both panels of 35 W were

manufactured for the experiments; the first was based on the standard manufacturing procedure and the second was developed with a 4 mm thick aluminum sheet having micro-channels of a cross-section of 1mm by 1 mm. They concluded that a temperature drops in 15 °C increments affect the power by 14% when a maximum water flow rate around 3 LPM was used. Babqi Abdulrahman J et al. [19] presented a performance investigation of the current model predictive control (CMPC) for a PV system with a two-stage transformer less control grid-connected under grid fault conditions. The CMPC strategy is to control the inverter output current connecting the utility grid to the PV system. In MATLAB/Simulink, the system and control strategy for the environment were simulated. In addition, comparative case studies were conducted between CMPC, PI, and Sliding Mode Control (SMC) under the network fault to validate the capability of the CMPC. Wei An et al. [20] presented a technique that was redesigned using a synergistic design strategy to overcome the flaws of the previous experiment systems. In an improved hybrid photovoltaic/distillation (PV/D) solar collector with a nanofluid-based spectral, gold nanofluid plays a dual role as a heat absorption medium and a spectral splitting filter to enhance the distillation of water. This system can maximize the utilization of solar energy in the whole spectrum and can obtain electricity and freshwater simultaneously. Mesude Bayrakci et al. [21] presents a new method for extracting roof segments and locating suitable areas for PV systems using Light Detection and Ranging (LIDAR) data and building footprints. Rooftop segments are created using seven slopes (tilt), aspect (azimuth) classes, and six different building types. Moreover, direct beam shading caused by nearby objects and the surrounding terrain is considered on a monthly basis. Finally, the method was implemented as an ArcGIS model in Model Builder and a tool was created. In order to show its validity, the method was applied to the city of Philadelphia, PA, USA with the criteria of slope, aspect, shading, and area used to locate suitable areas for PV system installation. Among the defects that damage the proper functioning of a solar station in desert environments, the MC4 connectors fail to electrically connect the photovoltaic modules [22]. This connector is simple; it consists of a flexible male (multi-blades contact) and a 4 mm cylindrical female that was developed and delivered in 2002 [23].

Arévalo Paul et al. [29] presents a novel photovoltaic power smoothing method in combination with moving averages and ramp rates to reduce fluctuations with hybrid storage systems (supercapacitors/batteries), and the main novelty involves optimizing the number of charging/discharging cycles under PV failures. To achieve this goal, a photovoltaic failure detection method is proposed that uses machine learning to process big data by monitoring the behavior of the photovoltaic. The results show a reduction for the supercapacitor operation with respect to other power smoothing methods. Moreover, the monitoring system can detect a failure in photovoltaic systems with a root mean squared error of 0.66 and the computational effort is reduced using the new smoothing technique. In this sense, the initial execution time is 4 times lower compared to the moving average method.

Benavides Dario et al. [30] presents a novel power smoothing method (predictor-corrector) using supercapacitors for a grid-connected photovoltaic system, with a method consisting of two stages: prediction and correction. The main novelty of the method is the use of a simple k-means algorithm application model in the cycle estimation stage for supercapacitors, with the aim of selecting representative data of power fluctuations and supercapacitor charge/discharge cycles. Then, for the correction stage, the novel proposed method uses ramp rate algorithms to generate the reference signal to control the charge state of the supercapacitor. According to the bibliographical study carried out in this research area, no studies were found that demonstrate the phenomenon of

degradation of the energy efficiency of solar stations due to the failure of the connectors between photovoltaic modules.

It is essential to say that the types of connectors used differ, and therefore the failure observed concerns only the connectors used in the solar station. The main objective of the work is to experimentally confirm the impact of the environmental factors (high ambient temperature and strong wind blowing sand) on the failure of connectors, which can cause a decrease, rupture, or shut-off of the station's energy production. The performance of other types of connectors under the same environmental conditions can be the focus of another study.

In this study, we will shed light on the aggressive effect of a blowing sandstorm in the presence of high temperature on the photovoltaic inter-module connectors in a solar stationlocated in the desert environment of southwestern Algeria (the station photovoltaic solar system of Kaberten-Adrar (Figure 1)).

Figure 1. The solar photovoltaic station Kaberten-Adrar.

The monitoring of the energy produced by the Kaberten-Adrar station showed a remarkable deterioration of this for the year 2021 compared to the year 2020, despite the station being still in the guarantee period. The detail of degradation showed that this phenomenon occurred during the months when the temperature was quite high (months of May, June, July, and August). The degradation rates recorded in the month in May 2021 compared to the same month of the year 2020 are given in the table below:

Table 1. Detailed energy degradation of Kaberten station production.

	Energy produced	Loss rate (%)	Degraded MC4 temperature (°C)	Temperature of MC4 no degraded (°C)	Radiant energy	Reduction rate of radiation (%)	Performance index (%)
May 2020	389,250 MWh	/	/	/	660 kWh	/	61
May 2021	360,900 MWh	–7.28	Min : 33.5 Max : 68.7	Min : 30.1 Max : 30.1	624 kWh	–5.52	59.9

The other solar stations in the Adrar area (Reggan, Aoulef, Zaouit-Konta station, etc.) were not affected by this degradation phenomenon because the Kaberten area is characterized by a quite high sand wind deposit displayed in Figure 2:
Ws: Wind speed in m/s.

Ws gust: Maximal measured wind speed within the time interval.
WD: Wind speed direction in N to East.
WD St Dev: Standard deviation of wind speed within measurement interval.

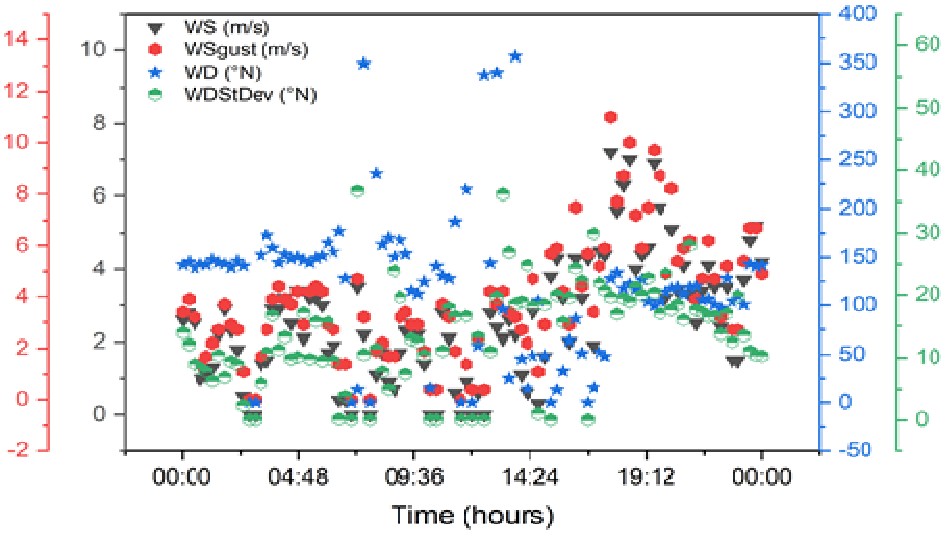

Figure 2. The wind speed Adrar.

While temperature growth is a common factor (Figure 3):

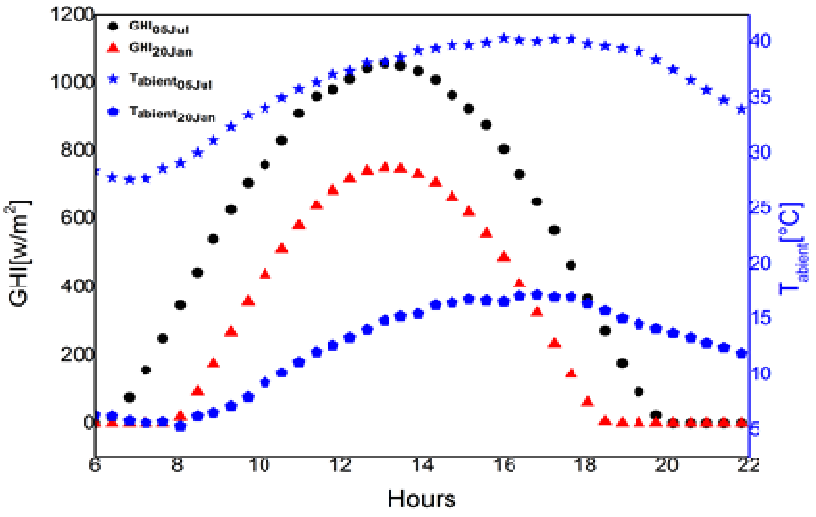

Figure 3. The ambient temperature and the overall horizontal radiative flux intensity.

A thermal camera photograph of the material of MC4 connector fails in the sequence of the photovoltaic modules of the Kaberten station showed the high temperature gradient compared to the normal connector, as displayed in Figures 4 and 5:

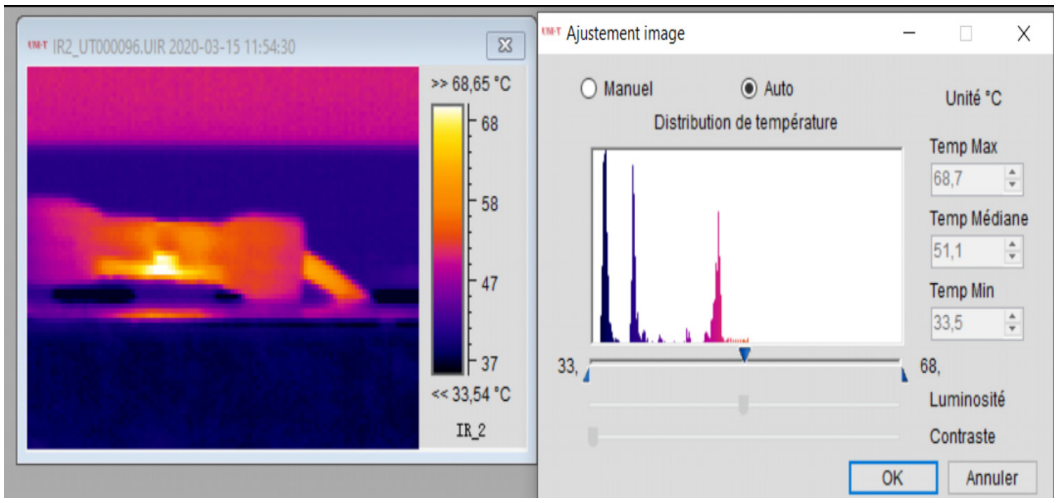

Figure 4. Thermographic image of the failed MC4 connector.

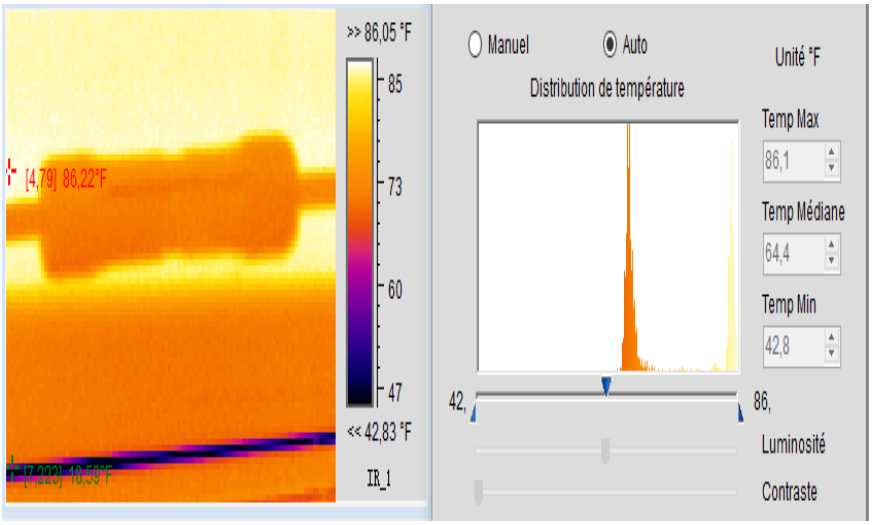

Figure 5. Thermographic image of no failed MC4 connector.

2. Materials and methods

To confirm the responsibility of dust (sand grains) and high temperatures on the failure of the MC4 connectors in the concerned photovoltaic station, we will use two new Am phenol connectors (Figure 6):

Figure 6. Amphenol connectors [22].

Table 2. Characteristics of Amphenol connectors.

Insulation material	PPO
Rated voltage	TUV 1000 DC/UL 600 V CC
Test voltage	6 KV (50 Hz, 1 min)
Contact material	Copper, tinned
Contact resistance	Less than 0.5 m Ohm
Degree of protection	IP67
Pollution degree	2
Protection class	Class II
Flame class	UL94-V0
Power take-off	Less than 50 N
Withdrawal force	More than 50 N
Ambient temperature range	–40 ~ + 90
Compatible with solar cable sections	2.5 mm², 4.0 mm² and 6.0 mm² (14 AWG, 12 AWG, 10 AWG)

We dip one of the two connectors into the sandbag and call them (Figure 7):

- ✓ MC1 sanded connector
- ✓ MC2 connector no sand

Figure 7. Sandblasted connector.

Then, we link the ends of each connector with cables in a solar station connected to the photovoltaic modules.

We connect the ends of these cables to a series circuit that contains the following: a shunt resistor of resistance:

$$R_{sh} = 0.002\Omega \tag{1}$$

And a voltage lamp

$$V_L = 24V(DC) \tag{2}$$

Then, the two branches in series are connected in parallel to a power source of 24 V (DC). Finally, we obtain an electrical circuit that contains the two connectors, MC1 and MC2, in parallel.

The shunt resistors in the two branches of the circuit are used to understand the current flowing through the terminals of each connector.

Then, we attach a thermocouple to each connector to monitor its temperature.

Finally, the two connectors, MC1 and MC2, were thrown into a thermal oven used to change the external temperature of the connectors (environmental temperature) and to prevent the intervention of any other environmental factor (humidity, solar radiation).

The different elements of the experiment are displayed in Figure 8.

Figure 8. experimental benches.

Figure 9 displays a representative diagram of the experiment described above.

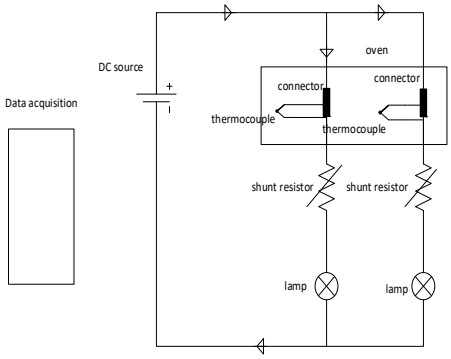

Figure 9. Representative diagram of the experiment.

After the calibration of the measuring devices according to the ISO/CEI 98-4:2012(E) [26] standards, and during three successive weeks, we checked for any variations of the intrinsic temperatures of each connector using the thermocouple for the three cases of the environmental temperatures (oven temperature). The voltages across the shunt resistors were also measured to calculate the currents flowing through each connector. Moreover, these measurements are processed during data acquisition. Finally, the powers dissipated in each branch of the circuit were calculated.

Figure 10 shows the electrical diagram of the experiment.

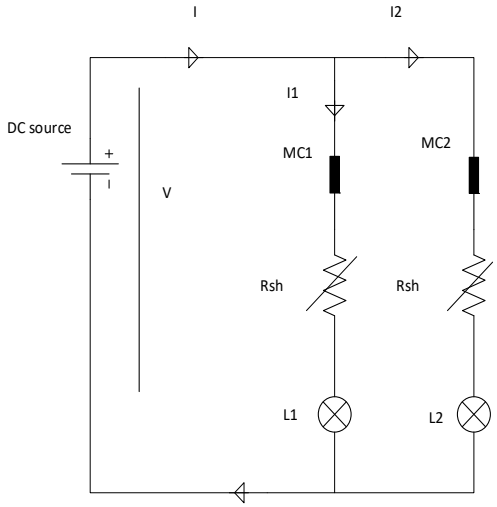

Figure 10. Electrical diagram of the experiment.

3. Results and discussion

The oven temperatures used were 50 ℃, 60 ℃, and 70 ℃, since these values represent the thresholds reached in the desert environment of Kaberten.

Table 3. Summaries the results obtained.

Connector			MC1	MC2
Temperature	50 ℃	P(W)	48	53
		U(V)	0.0040	0.0044
		I(A)	2.00	2.21
		P_1(W)	5	0
	60 ℃	P(W)	47.5	52
		U(V)	0.0039	0.0043
		I(A)	1.98	2.17
		P_1(W)	5.5	1
	70 ℃	P(W)	47.4	52
		U(V)	0.0039	0.0043
		I(A)	1.94	2.18
		P_1(W)	5.6	1

Such as:
P: power supplied in the branch of the connector,
P_1: Power dissipated in the connector leg, and
U: voltage measured at the shunt resistor terminal.
It has well known that:

$$I = \frac{U}{R} \tag{3}$$

and

$$P = U \times R \tag{4}$$

In addition:

$$I = I_1 + I_2 \tag{5}$$

where:

- I_1: is the current through the MC1 sanded connector,
- I_2: Current through the no sand MC2 connector,
- R_L: The resistance of the lamp,
- P_{11}: Power dissipated in the branch of the connectors MC1, and
- P_{12}: Power dissipated in the branch of the connectors MC2.

The power dissipated in the sanded connector and unsanded connector:

$$P_{MC1} = R_{MC1}.I_1^{\,2} \tag{6}$$

and

$$P_{MC2} = R_{MC2}.I_2^{\,2} \tag{7}$$

With the three oven temperatures used, the current flowing through the MC2 connector is greater than that flowing through MC1.

$$I_2 \succ I_1 \tag{8}$$

It is obvious from the above formulas that:

$$R_{MC1} \succ R_{MC2} \tag{9}$$

This implies that the power dissipated in the sanded connector (MC1) is greater than the power dissipated in the no sand connector (MC2),

$$R_{MC1}I_1^2 \succ R_{MC2}I_2^2 \tag{10}$$

- The characteristics of the lamps are identical (24 V/50 W)
- The connector contact resistance is 0.0005 Ω (see Table 2)
- Both branches are parallel so the same voltage 24 V

To calculate the resistance of the MC1 and MC2 connectors, we use the data in Table 3 and use Formulas 8 and 9:

$$P_{11} = R_{MC1}I_1^2 \tag{11}$$

$$P_{12} = R_{MC2}I_2^2 \tag{12}$$

We record the result in the table below.

Table 4. Resistor of the sanded connector and connector no sand.

Oven temperature	R_{MC1} (Ω)	R_{MC2} (Ω)
At 50 ℃	1.25	0
At 60 ℃	1.40	0.212
At 70 ℃	1.48	0.210

At its core, tinned copper consists of two elements: copper and tin. Copper is an incredibly versatile metal that's highly conductive, meaning it absorbs and transfers electricity very quickly. Tin acts as a protective agent for copper, providing resistance against corrosion and other environmental factors. The combination of these two metals creates a durable alloy that can withstand extreme temperatures and high levels of stress without breaking down or losing its conductivity.

Tinned Copper Properties R_MC2 (Ω):

Tinned copper has some remarkable properties that make it ideal for use in various industrial applications. First, it's highly malleable, meaning it can be bent or molded into any shape without compromising its strength or durability. Additionally, since the tin serves as a protective layer for the underlying copper, this alloy also has excellent corrosion resistance, even when exposed to either harsh chemicals or salty sea air. Finally, tinned copper has superior thermal conductivity compared to other metals like aluminum or steel, making it an ideal choice for applications where heat needs to dissipate quickly and efficiently [22].

In order to interpret the increase in resistance of the sandblasted connector compared to the unblasted connector, we know that Matthiessen's model shows that the resistivity of conductive alloys decreases when the temperature increases, in fact:

$$\rho = \rho_T + \rho_I + \rho_D \tag{13}$$

where

ρ_T: contribution of thermal agitation,

ρ_I: contribution of impurities, and

ρ_D: contribution of atomic defects.

Indeed, thermal agitation presents the kinetic energy that the electrons yield to the lattice at each collision (the Joule effect).

The Drude model presents the resistivity of a metal (or alloy of metals) at a given temperature:

$$\rho = \rho_0(1 + \alpha t) \tag{14}$$

where

ρ_0: resistivity at reference temperature (Ωm),

α: temperature coefficient (K−1), and

t: temperature (K°).

Semiconductors manifest as conductors when they receive sufficient thermal energy, and the induced current is given by the following equation [27]:

$$I = f\left(\left[\frac{2\pi KT}{h^2}\right]^3\right) \tag{15}$$

When the sandblasted connector (MC1) becomes hotter, the electronic collisions increase, this means that the shocks of the electrons in the connector and the shocks of the electrons of the sand/semiconductor both increases. Therefore, it makes sense that the sandblasted connector becomes more resistive than the undblasted connector at a high ambient temperature.

The figures below show the variation of the internal temperature of each connector as a function of time.

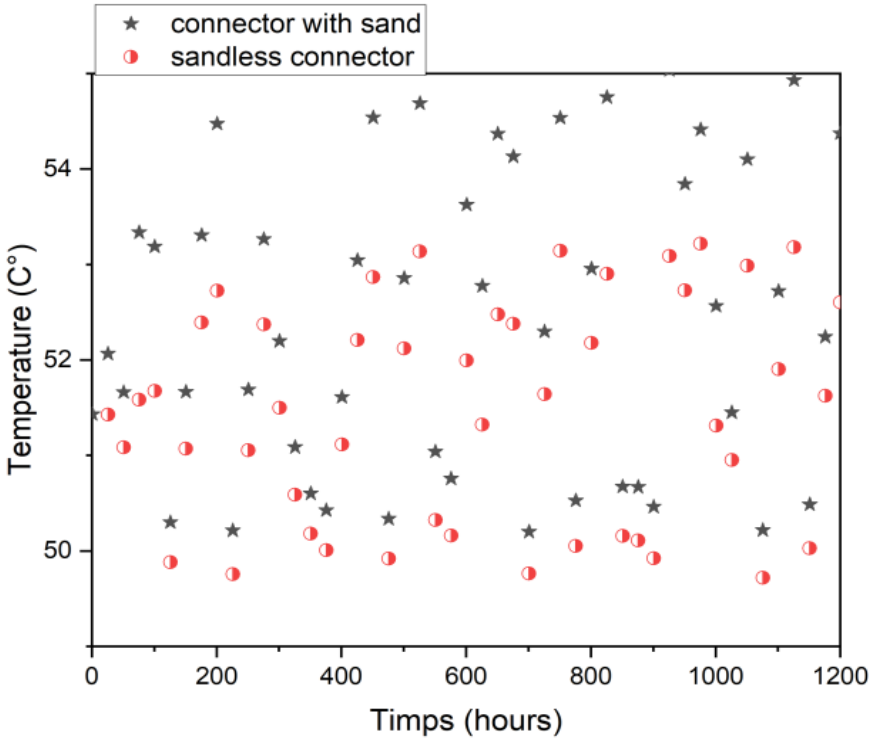

Figure 11. MC1 and MC2 temperatures at oven temperature 50 °C.

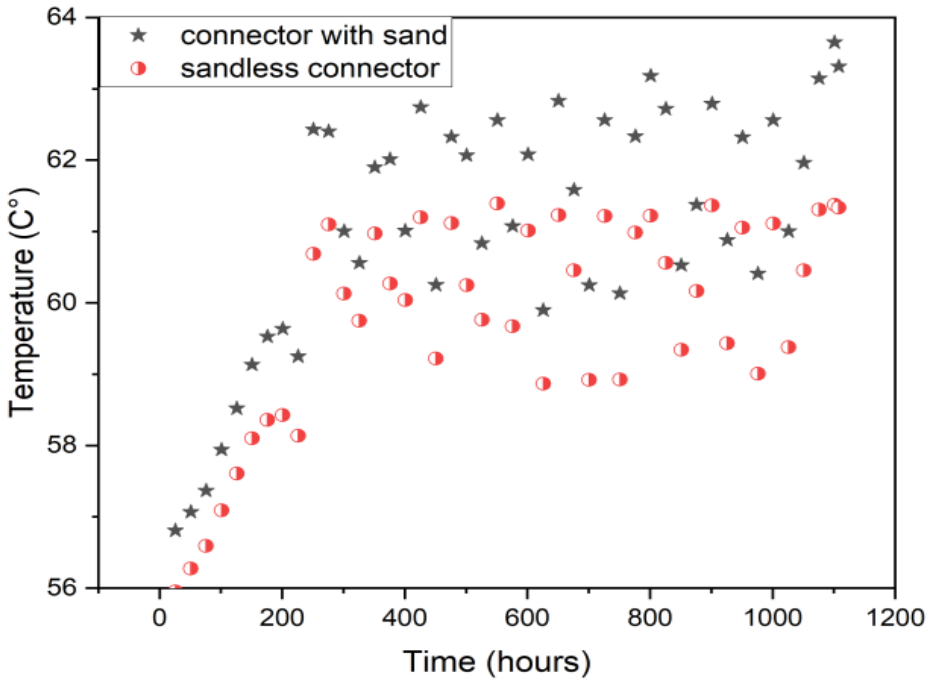

Figure 12. MC1 and MC2 temperatures at oven temperature 60 °C.

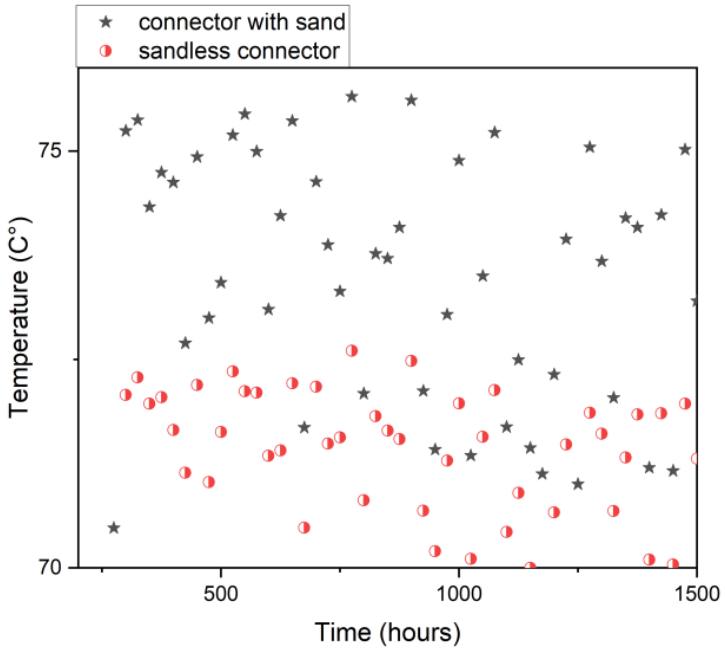

Figure 13. MC1 and MC2 temperatures at oven temperature 70 °C.

We observe from these graphs that the MC1 connector always remain warmer than the MC2 connector, which implies that MC1 becomes very resistive, and thus the dissipation of power becomes important.

Similarly, we present the voltage variations at the terminal of the shunt resistor and the power variations at the terminal of each branch of the circuit for the different cases of furnace temperature in Figures 14–20.

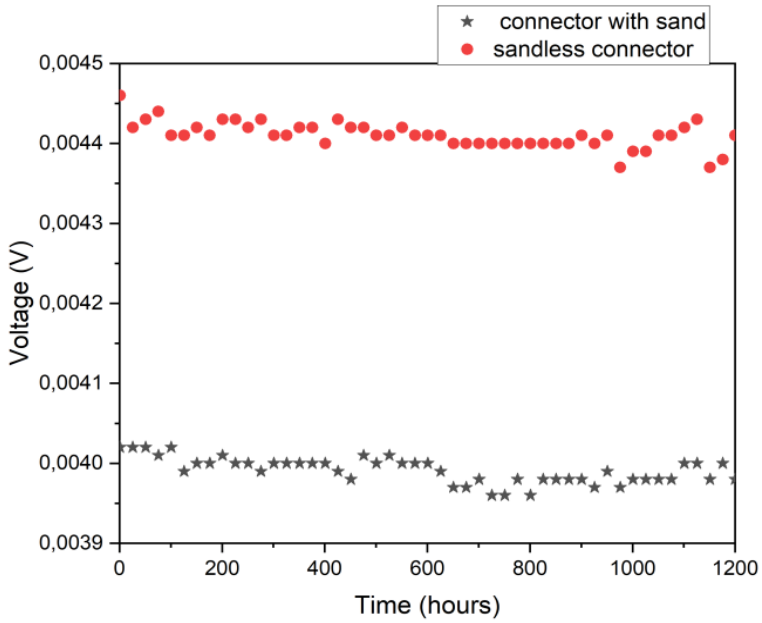

Figure 14. Voltage across the shunt resistors in the two branches of the circuit (MC1 and MC2) at 50 ℃.

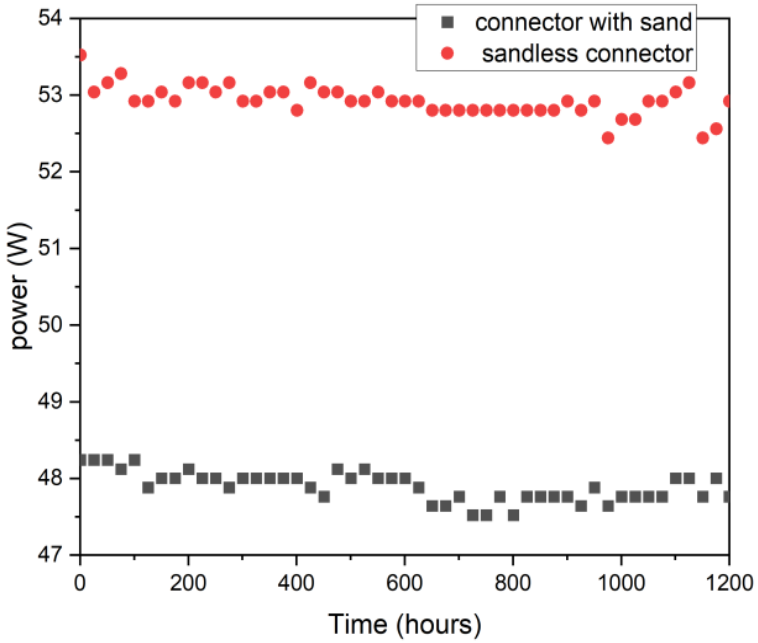

Figure 15. Power supplied in the two branches of the circuit (MC1 and MC2) at 50 ℃.

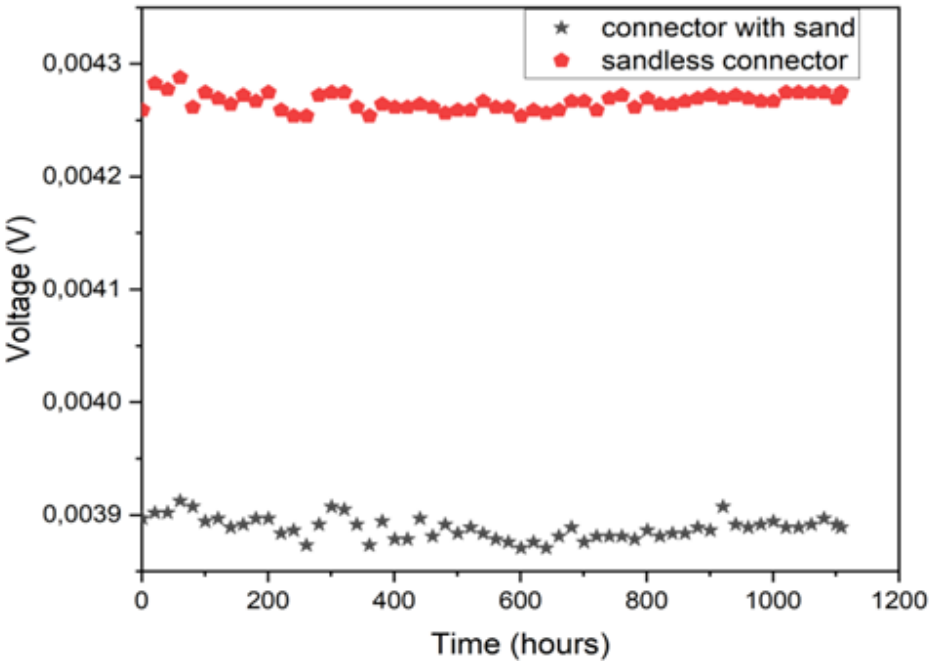

Figure 16. Voltage across the shunt resistors in the two circuit branches (MC1 and MC2) at 60 ℃.

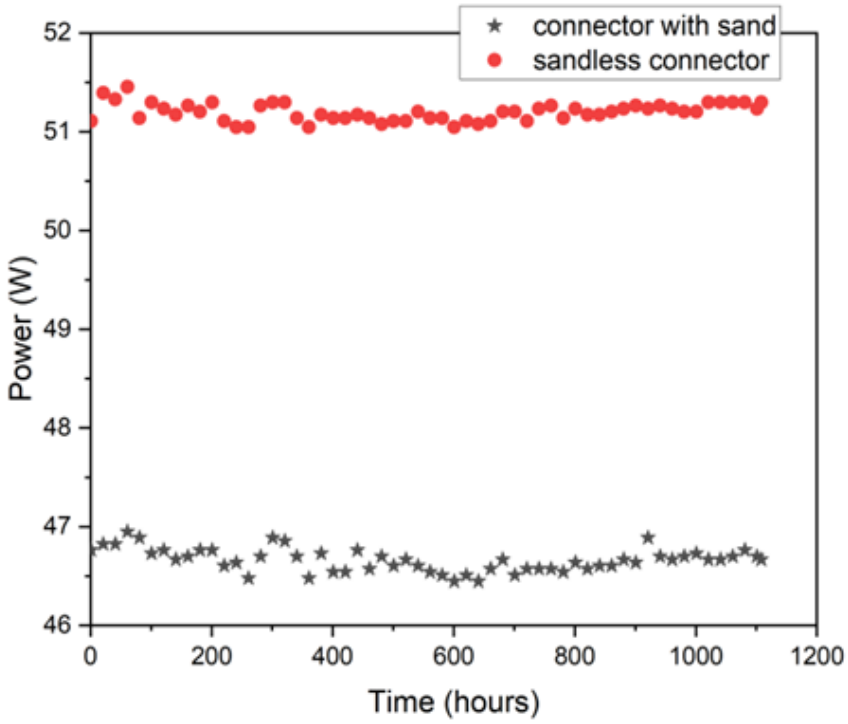

Figure 17. Power supplied in the shunt resistor in both cases (MC1 and MC2) at 60 ℃.

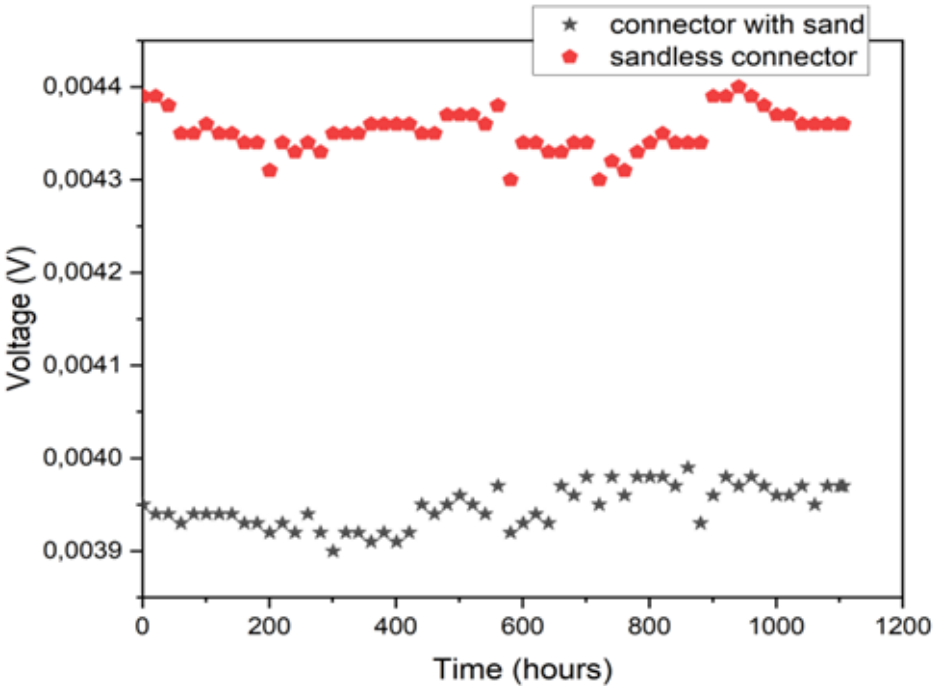

Figure 18. Voltage across the shunt resistors in the two circuit branches (MC1 and MC2) at 70 ℃.

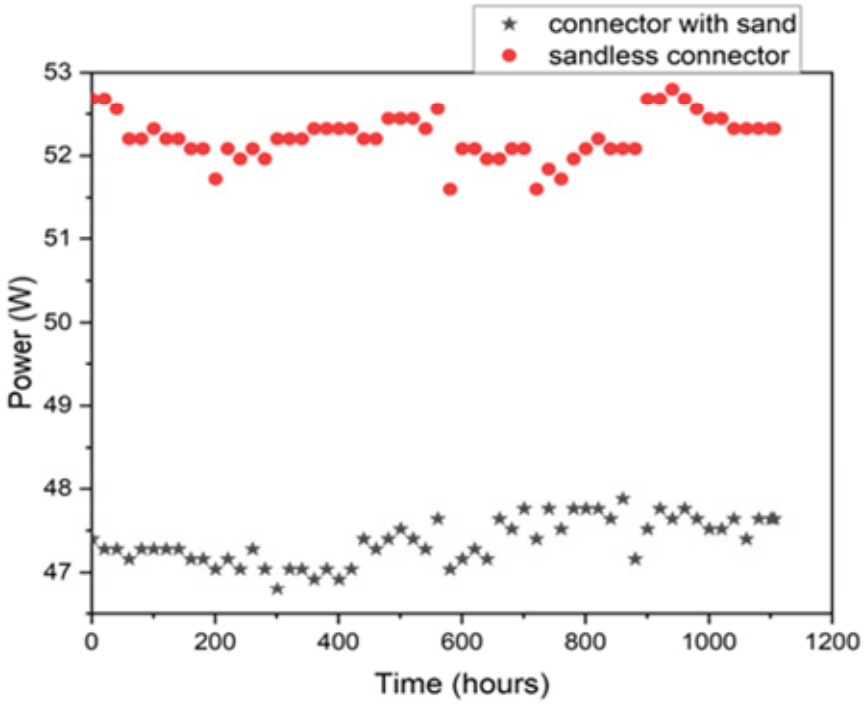

Figure 19. Power supplied in the shunt resistor in both cases (MC1 and MC2) at 70 ℃.

The difference in power dissipation in the two branches containing the two connectors MC1 and MC2 is shown in Figures 22–24.

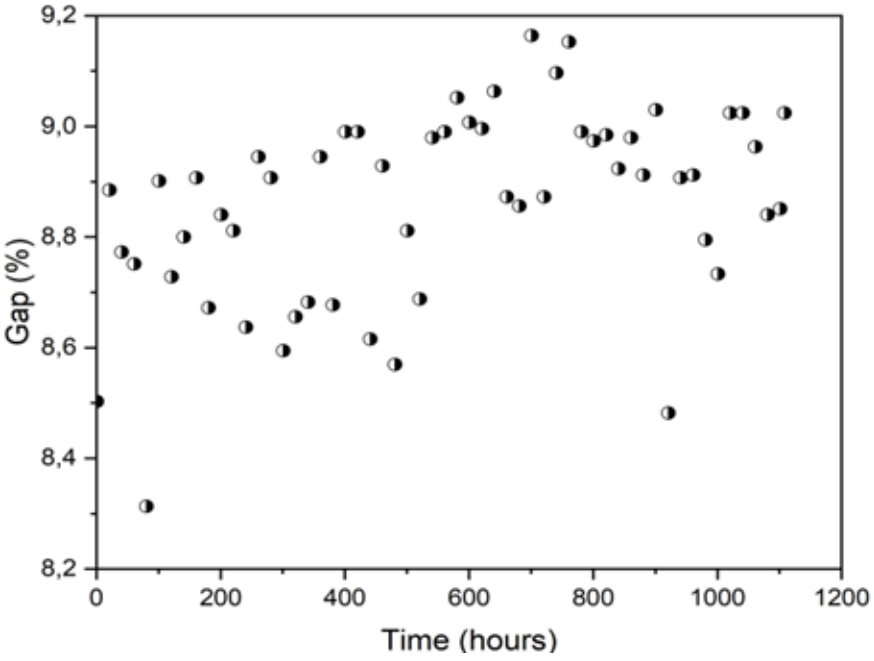

Figure 20. Power supplied difference in the two connectors MC1 and MC2 at 50 ℃.

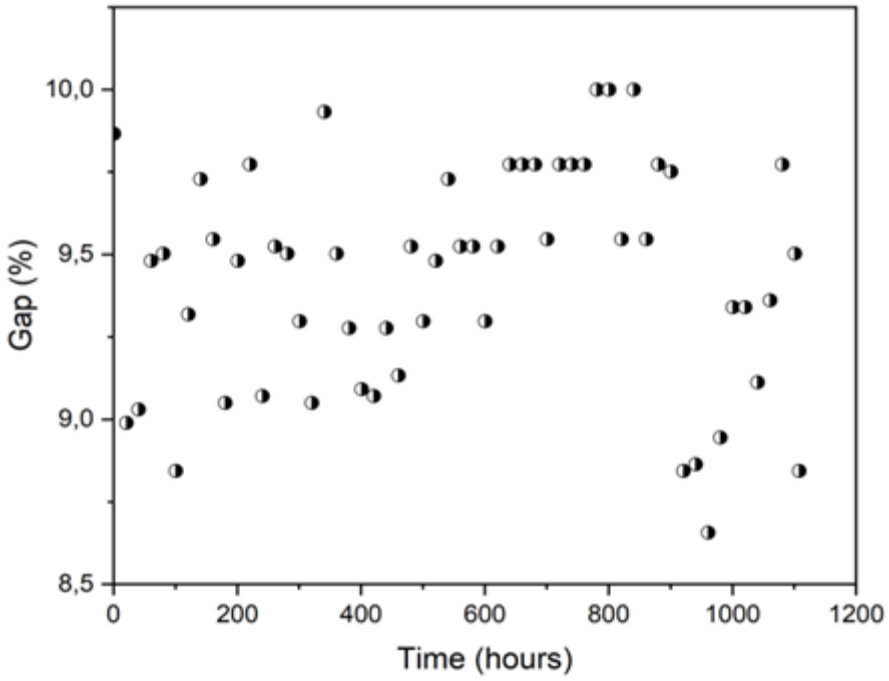

Figure 21. Power dissipation difference in the two connectors MC1 and MC2 at 60 ℃.

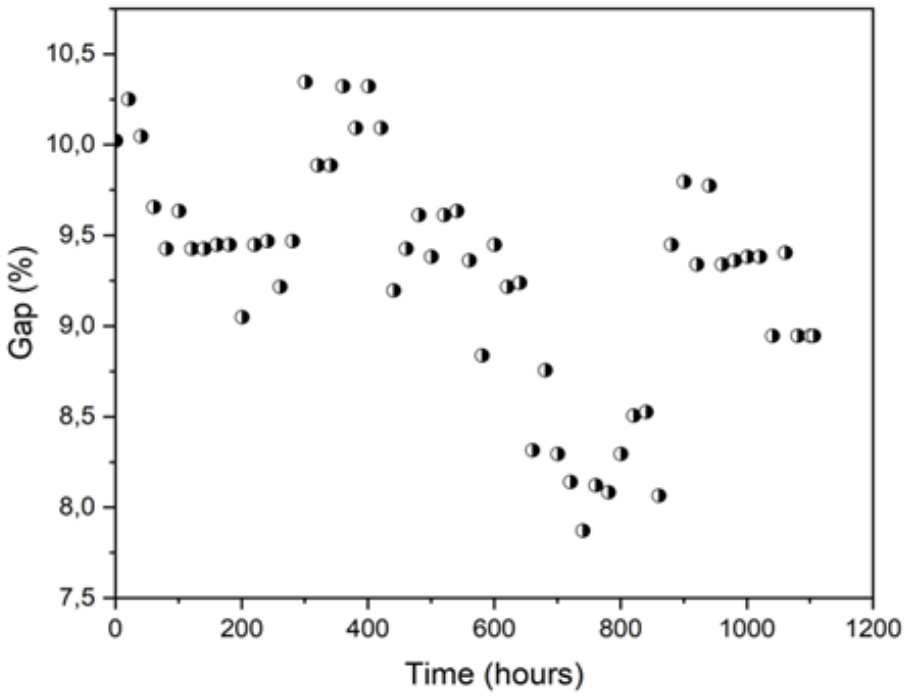

Figure 22. Power dissipation difference in the two connectors MC1 and MC2 at 70 ℃.

The figures above clearly show the high-power dissipation in the sandblasted connector compared to the sand less connector, with a difference of up to 10%.

Our results present a good agreement with a computer simulation regarding critical thermal points of electrical installations presented by Szultka et al. [28] and the photovoltaic power smoothing method presented by Arévalo et al. [29].

The connectors temperature limit equal to 105 ℃, which is important for the safety of people and buildings.

4. Conclusions

This work is a study of the effect of dust (grains of sand) and high temperature on the connectors linking the photovoltaic modules in a photovoltaic solar station located in a desert environment, characterized by the blowing of the sand winds at fairly high speeds in periods of the year when the temperature is also quite high. In this situation, the heat produced in the connectors accelerates their complete failure, effectively lowering the station's energy efficiency. We emphasize that this phenomenon was not observed before the temperature exceeded the value of 50 ℃. For a period of four months, the power loss of the Kaberten station reaches 10% of the Nameplate Capacity. This annual energy loss was more than 360 MWh. In addition, this phenomenon leadsto the destruction of the connectors, and therefore ceases the operation of the station. Regardless of the connector type used, the study demonstrated the logical decrease of conductivity of the conductors due to sand grains entering their protective cover in the presence of a high ambient temperature. Therefore, ceasing the entry of sand grains should be the suggested solution.

Acknowledgments

The present work was effectuated in the Thermal and Thermodynamics Conversion Division, within the Research Unit in Renewable Energies in the Sahara Medium. Development Centre of Renewable Energies, Adrar, Algeria. We would like to express our deepest appreciation to the URERMS unit.

Conflict of interest

The PV station problematic detected in the largest Kaberten SKTM electricity and renewable energy companies in the south of Algeria.

The authors declare that they have no known competing financial interests or personal relationships that could have appeared to influence the work reported in this paper.

Use of AI tools declaration

No AI use in the document.

References

1. Daher D (2017) Modeling and experimental analysis of a photovoltaic solar power plant in a maritime desert environment. Thermal [physics.class-ph]. *University of Lyons.* Available from: https://theses.hal.science/tel-01920874/.
2. Sørensen B, Watt G (2006) Trends in photovoltaic applications, survey report of selected IEA countries between 1992 and 2005: Report IEA-PVPS T1-15:2006. *IEA Press.* Available from: http://www.iea-pvps.org/products/download/rep1_15pdf.
3. Maamar AT, Ladjouzi S, Taleb R, et al. (2018) Fault detection and classification for a GPV: Comparative study between the thresholding method and neural networks. *Renewable Energy Rev* 21: 45–53. Available from: https://www.cder.dz/download/Art21-1_6.pdf.
4. Gong YJ, Wang Z, Lai ZY, et al. (2021) TVACPSO-assisted analysis of the effects of temperature and irradiance on the PV module performances. *Energy* 227: 120390. https://doi.org/10.1016/j.energy.2021.120390
5. khanam S, Meraj Md, Azhar Md, et al. (2021) Comparative performance analysis of photovoltaic modules of different materials for four different climatic zone of India. *Urban Clime* 39: 100957. https://doi.org/10.1016/j.uclim.2021.100957
6. Ameur A, Berrada A, Bouaichi A, et al. (2022) Long-term performance and degradation analysis of different PV modules under temperate climate. *Renewable Energy* 188: 37–51. https://doi.org/10.1016/j.renene.2022.02.025
7. Takeguchi K, Nakayama K, Chantana J, et al. (2020) Spectral gain and loss of different-type photovoltaic modules through average photon energy of various locations in Japan. *Sol Energy* 214: 1–10. https://doi.org/10.1016/j.solener.2020.10.092
8. Aboagye B, Gyamfi S, Antwi EO, et al. (2021) Degradation analysis of installed solar photovoltaic (PV) modules under outdoor conditions in Ghana. *Energy Rep* 7: 6921–6931. https://doi.org/10.1016/j.egyr.2021.10.046

9. Singh R, Sharma M, Yadav K (2022) Degradation and reliability analysis of photovoltaic modules after operating for 12 years: A case study with comparisons. *Renewanle Energy* 196 : 1170–1186. https://doi.org/10.1016/j.renene.2022.07.048
10. Dahbi H, Aoun N, Sellam M (2021) Performance analysis and investigation of a six MW grid-connected ground-based PV plant installed in hot desert climate conditions. *Int J Energy Environ Eng* 12: 577–587. https://doi.org/10.1007/s40095-021-00389-x
11. Bouraiou A, Hamouda M, Chaker A, et al. (2018) Experimental investigation of observed defects in crystalline silicon PV modules under outdoor hot dry climatic conditions in Algeria. *Sol Energy* 159: 475–487. https://doi.org/10.1016/j.solener.2017.11.018
12. Boussaid M, Belghachi A, Agroui K, et al. (2016) Solar cell degradation under open circuit condition in out-doors-in desert region. *Results Phys* 6: 837–842. https://doi.org/10.1016/j.rinp.2016.09.013
13. Ali Sadat S, Faraji J, Nazififard M, et al. (2021) The experimental analysis of dust deposition effect on solar photovoltaic panels in Iran's desert environment. *Sustainable Energy Technol Assess* 47: 101–542. https://doi.org/10.1016/j.seta.2021.101542
14. Zhao W, Lv YK, Zhou QW, et al. (2021) Investigation on particle deposition criterion and dust accumulation impact on solar PV module performance. *Energy* 233: 121–240. https://doi.org/10.1016/j.energy.2021.121240
15. Jiang Y, Lu L, Lu H (2016) A novel model to estimate the cleaning frequency for dirty solar photovoltaic (PV) modules in desert environment. *Sol Energy* 140: 236–240. https://doi.org/10.1016/j.solener.2016.11.016
16. Benabdelkrim B, Benattilah A, Ghaitaoui T, et al. (2021) Experimental analysis of a photovoltaic power plant in a desert environment-Adrar area. *Algerian J Renewable Energy Sustainable Dev* 3: 85–96. https://doi.org/10.46657/ajresd.2021.3.1.9
17. Mohammad AT, Al-Shohani WA (2022) Numerical and experimental investigation for analyzing the temperature influence on the performance of photovoltaic module. *AIMS Energy* 10: 1026–1045. https://doi.org/10.3934/energy.2022047
18. Muzaffar A, Hafiz MA, Waqar M, et al. (2015) Performance enhancement of PV cells through micro-channel cooling. *AIMS Energy* 3: 699–710. https://doi.org/10.3934/energy.2015.4.699
19. Abdulrahman JB, Nasim U, Ahmed A, et al. (2022) Current model predictive fault-tolerant control for grid-connected photovoltaic system. *AIMS Energy* 10: 273–291. https://doi.org/10.3934/energy.2022015
20. Wei A, Yifan Z, Bo P, et al. (2021) Synergistic design of an integrated PV/distillation solar system based on nanofluid spectral splitting technique. *AIMS Energy* 9: 534–557. https://doi.org/10.3934/energy.2021026
21. Mesude B, Kirby C, Jeffrey R, et al. (2015) An automated model for rooftop PV systems assessment in ArcGIS using LIDAR. *AIMS Energy* 3: 401–420. https://doi.org/10.3934/energy.2015.3.401
22. Solar inverter and MC4 connectors. Available from: https://imeonenergy.com/accessoires/accessoires-onduleur-9-12/onduleur-solaire-connecteurs-mc4.
23. Photovoltaic connectivity: The MC4 and its cousins-Photovoltaic Forum. Available from: https://forum-photovoltaique.fr/viewtopic.php?t=32400.

24. Mohamed B, Fadela B, Mounir K (2015) Optimization of the wind turbines location in Kaberten wind farm in Algeria. *Energy Proc* 74: 122–129. https://doi.org/10.1016/j.egypro.2015.07.532
25. Adrar climate: Average temperature, weather by month. Available from: https://en.climate-data.org/africa/algeria/adrar/adrar-44519/#temperature-graph consulté le 21 mars 2023.
26. Puydarrieux S, Pou JM, Leblond L, et al. (2019) Role of measurement uncertainty in conformity assessment. *In 19th International Congress of Metrology (CIM2019), Paris, France* https://doi.org/10.1051/metrology/201916003
27. Boussaid M (2017) Mathematical models of the phenomenon of aging and degradation of photovoltaic cells and modules. *Ahmed Draia University, Adrar, Doctoral thesis.*
28. Szultka S, Czapp S, Tomaszewski A, et al. (2023) Evaluation of fire hazard in electrical installations due to unfavorable ambient thermal conditions. *Fire* 6: 41. https://doi.org/10.3390/fire6020041
29. Arévalo P, Benavides D, Tostado-Véliz M, et al. (2023) Smart monitoring method for photovoltaic systems and failure control based on power smoothing techniques. *Renewable Energy* 205: 366–383. https://doi.org/10.1016/j.renene.2023.01.059
30. Benavides D, Arévalo P, Aguado JA, et al. (2023) Experimental validation of a novel power smoothing method for on-grid photovoltaic systems using supercapacitors. *Int J Electrical Power Energy Syst* 149: 109050. https://doi.org/10.1016/j.ijepes.2023.109050

AIMS Press

© 2023 the Author(s), licensee AIMS Press. This is an open access article distributed under the terms of the Creative Commons Attribution License (http://creativecommons.org/licenses/by/4.0)